Possibilities for treating produced water with ceramic membranes

Additional Thesis

Author: Hanxiao Zhou (5463637)

Supervisor: dr. ir. S. G. J Heijman, Associate professor

Ir. Guangze Qin, PhD student

Content

1. Introduction

Oily water emulsions are generated by industrial sources and mainly include salt and hydrocarbons which are toxic to the environment (Cui et al., 2008; Hua et al., 2007; Mohammadi et al., 2003), then membrane filtration, heating treatment, electrostatic coalescing, pH adjustment, gravity settling, centrifugal settling, filter coalescing, and chemical emulsification were used to treat oily wastewater (Cui et al., 2008; Mohammadi et al., 2003). However, these techniques have been found to have some drawbacks, including high costs, a need for a lot of space, and the production of secondary pollutants (Zhou et al., 2010). Membrane separation techniques are becoming more popular as cutting-edge technological solutions for wastewater because they are rather energy-efficient, economical, and environmentally friendly (Panpanit et al., 2000).

Most studies on the use of polymeric and ceramic membranes for the treatment of oily wastewater concentrated on using ultra-filtration (UF) and microfiltration (MF) methods (Abadi et al., 2011; Barredo-Damas et al., 2010). Ceramic membranes are always preferred to polymeric membranes for industrial application due to higher selectivity, significant permeation rate, superior chemical and thermal stability, and, most importantly, longer lifetime (Ding et al., 2006; Pugazhenthi et al., 2005). The undesirable foulant deposition on the membrane surface, which reduces treatment rate, decreases permeance and increases energy use, is the main disadvantage of membrane separation technology (Chen et al., 2022; Ullah et al., 2021).

The majority of oil-in-water (O/W) emulsions have oil droplet sizes that range from tens of nanometers to hundreds of micrometers. The majority of currently conducted studies have mainly been concerned with treating emulsions containing micron-sized oil droplets, for which most ceramic membranes exhibit 90–99% rejection (Chen & Liu,

2020; Tanudjaja et al., 2019). However, since nano-sized oil droplets have smaller size and higher colloidal stability, so it is more challenging and difficult to separate. Separation of nano-sized O/W emulsions using robust ceramic membrane has been rarely reported, and the comparison of different ceramic membranes on treating nano-sized O/W emulsions as well as factors on affecting membrane fouling should be further explored.

Constant flux MF/UF filtration is preferred in real-world applications because it provides more consistent permeate flow rates than fixed transmembrane pressure (TMP) studies. Particularly, little is understood about the fouling of ceramic membranes in constant flux filtration modes by nano-sized O/W emulsions.

In this study, the effects of emulsion chemistry containing pH, different surfactants, as well as salinity on the alumina and SiC deposited ceramic UF membranes with various physicochemical surface properties in the constant flux mode were compared.

This study seeks to provide answers to the following three research questions considering the knowledge gap and research objectives:

1) What is the influence of pH on the fouling of Al_2O_3 and SiC-deposited ceramic membranes?
2) How surface charge of Al_2O_3 and SiC-deposited ceramic membranes affect the separation of nano-sized O/W emulsions stabilized with different surfactants?
3) What is the influence of different salinity on the fouling of Al_2O_3 and SiC-deposited ceramic membranes?

The research questions' hypotheses are as follows:

1) With an increase in pH, fouling on both membranes is reduced. When compared to the Al_2O_3 membrane, fouling on the SiC-deposited membrane is always lower.

2) The Al_2O_3 membrane has less fouling when dealing with nano-sized O/W emulsions stabilized with Span 80/cetrimonium bromide (CTAB), while the SiC-deposited membrane has less fouling when dealing with nano-sized O/W emulsions stabilized with Span 80/sodium dodecyl sulfate (SDS), as well as Span 80/Tween 80.
3) The fouling of both membranes becomes higher when NaCl concentration increases from 1mM to 10mM, and the fouling of the SiC-deposited membrane is less. When 1 mM $CaCl_2$ is added to the emulsions, the membrane fouling becomes worse compared with emulsions with 1 mM NaCl.

A literature review and laboratory experiments were conducted to answer the aforementioned research questions and validate the hypotheses.

2. Literature review

2.1 O/W emulsions

Oil in oily wastewaters can be divided into three categories: dissolved oil (less than 0.5 wt %), emulsified oil (about 10 wt %), as well as floated oil and dispersed oil (about 90 wt %) (Stewart, 2009), then the emulsified oil is referred as the O/W emulsion. Since the emulsified oil (<10μm) is stabilized by surfactants, which significantly lower the interfacial tension between oil and water, the tiny oil droplets are challenging to remove (Janknecht et al., 2004). In contrast, large droplet sizes (>10μm) of floating and dispersed oil make them mechanically easy to remove (Lu et al., 2015). Micron-sized O/W emulsions can be separated using microfiltration and ultrafiltration at TMP as low as 0.1-2 bar for MF and 1-5 bar for UF as well as high flux rates (Mulder & Mulder, 1996).

In some industrial processes, oily wastewaters with nano-sized oil droplets (2-200 nm) are common (Fakhru'l-Razi et al., 2009; Hu et al., 2015). Although there have been some studies on the use of cellulose-based carbon and polymeric membranes (Hu et al., 2019; Li et al., 2019) as well as carbon nanotubes (Hu et al., 2015) to treat nano-sized O/W emulsions, rare reports have been made of the separation of nano-sized O/W emulsions using more durable ceramic membranes.

2.2 Ceramic membranes for nano-sized O/W emulsions separation

Over the past 30 years, membrane separations have been advanced significantly and are now a promising technology (Abadi et al., 2011). Compared to conventional treatment methods, they are more effective at removing oil, use less energy, and have a smaller design. The ability to achieve the current regulatory treatment goals without chemical pretreatment is the main benefit of using ceramic membranes (Ebrahimi et al., 2010; Hua et al., 2007).

In recent years, organic membranes, especially MF, UF and reverse osmosis (RO), have been used for separation for oily wastewater treatment (Barredo-Damas et al., 2010; Ebrahimi et al., 2009; Mohammadi et al., 2003), while ceramic membranes have higher fluxes because of their higher porosity and more hydrophilic surface compared with organic membranes (Abadi et al., 2011). Moreover, ceramic membranes are more durable when used in high-temperature and corrosive environments than polymeric membranes because of their mechanical, chemical, and thermal stability (Chen et al., 2017; Chen et al., 2016). Furthermore, after severe fouling, ceramic membranes can be chemically cleaned in harsh conditions to restore their performance. In industrial applications, this can also increase their service lifetime (He & Vidic, 2016). Hence, ceramic membranes could be useful and efficient to remove O/W emulsions in water.

Recently, Wang et al. (2022) used robust zirconia ceramic membrane for purifying nano-emulsion oily wastewater in constant pressure filtration mode, and Liu (2022) used alumina UF membranes to treat nano-sized O/W emulsions in the constant flux filtration mode as well as investigated the effects of four different factors on membrane fouling, including membrane pore size, cross flow velocity, pH, and salinity. They provided a promising way to treat nano-sized O/W emulsions by robust ceramic membranes while the separation performance of the membrane could still be further improved, thus this study aims to explore whether the SiC-deposited membrane has better separation performance of nano-sized O/W emulsions compared with the Al_2O_3 membrane.

2.3 Al_2O_3 ceramic membranes and SiC-deposited ceramic membranes

SiC membranes show lower reversible and irreversible fouling for surface water and, especially, produced water treatment when compared to other ceramic and polymeric membranes because of surface properties that combine super-hydrophilicity and a highly negative charge (He & Vidic, 2016; Hofs et al., 2011). Ceramic membranes made of SiC are particularly important for wastewater treatment because of their durability, chemical stability, and antifouling properties (Chen et al., 2020). The alfa-Al_2O_3 ceramic membranes are very inert chemically and they are functional between pH values of 1 and 14, so there are no restrictions on temperature or pH when using conventional membrane cleaners (Abadi et al., 2011). Chen et al. (2022) found that the SiC-deposited membranes had smaller average pore sizes and a narrower pore size distribution than the original Al_2O_3 membrane.

Al_2O_3 ceramic membranes and SiC-deposited ceramic membranes both have hydrophilic surfaces, but their isoelectric points (IEP) differ from each other. SiC has

been found to have a low IEP (2–3), while Al_2O_3 typically has a high IEP (8–9) (Xu et al., 2020). As a result, in a neutral environment (pH = 5.6), the surface charges of the two membranes would be opposite, which could result in various fouling mechanisms. For O/W emulsion filtration, the SiC-deposited membrane was less prone to fouling than the Al_2O_3 membrane since the former had the less reversible and irreversible fouling resistance than that of the latter (Chen et al., 2020).

2.4 Fouling mechanisms in membrane separation

One of the main operational issues is the fouling of the membranes, which drives up the cost of running the membranes and decreases the filtration flux, as well as reduces the membrane life (Yu et al., 2019), so it is crucial to explore the fouling mechanisms in membrane separation. Despite the growing interest in ceramic membranes for the water treatment, there is little information available about fouling behaviors in this setting.

The membrane fouling could be divided into reversible fouling and irreversible fouling. When filtering oily wastewaters, irreversible fouling frequently happens, significantly reducing permeate flux. The main causes of irreversible fouling are (1) intense foulant adsorption on membrane surface and pores, and (2) foulant blockage inside membrane pores, both of which are very challenging or impossible to recover with hydraulic back flush (Zhou et al., 2010). The life of the membrane is ultimately shortened by severe irreversible fouling, which necessitates frequent chemical cleaning. Reversible fouling is primarily attributed to the accumulation and deposition of foulants on the membrane surface during the filtration of oily wastewater (Chen et al., 2009), and permeance decline could be easily reversed by hydraulic washing techniques like cross flush and back flush.

Understanding of membrane separation processes has improved significantly because of modeling membrane fouling. Complete pore blocking, intermediate pore blocking, standard pore blocking, and cake filtration (Figure 1) are four different fouling mechanisms in constant pressure dead-end filtration (DEF) that Hermia developed equations to describe (Hermia, 1982). Despite the fact that many practical membrane separations are carried out in this way, there is little modeling of fouling mechanisms in constant flux crossflow filtration (Committee, 2008). Complete pore blocking and standard pore blocking were ruled out of consideration due to competing assumptions and relevance, however, a model combining intermediate pore blocking and cake filtration seemed to provide the best agreement with the experimental results of the constant flux crossflow ultrafiltration (Kirschner et al., 2019).

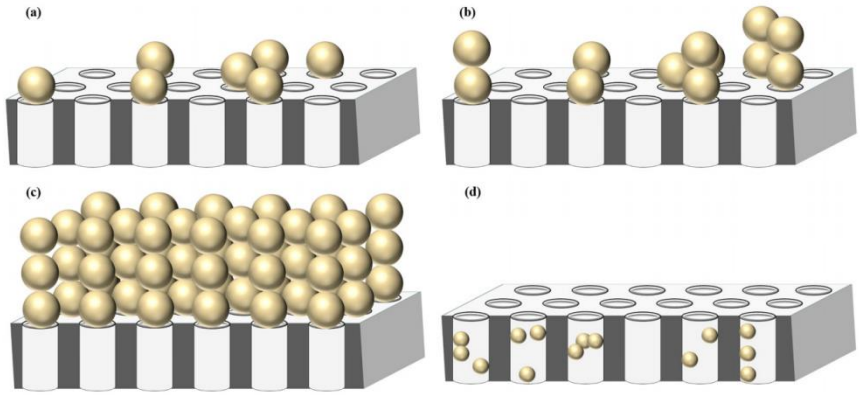

Figure 1. The fouling mechanisms of Hermia are depicted schematically as follows: (a) Complete pore blocking, (b) Intermediate pore blocking, (c) Cake filtration and (d) Standard pore blocking (Hermia, 1982; Kirschner et al., 2019)

Kirschner et al. (2019) also demonstrated that the gradual increase in TMP with filtration time in the later stages of the experiment suggests that the foulant cake keeps growing indefinitely and proposed that the threshold flux is the flux above which cake filtration becomes the predominant fouling mechanism and below which cake buildup is negligible.

2.5 Influential factors in the constant flux crossflow filtration

2.5.1 pH

Fresh O/W emulsions naturally have a pH of 5.6, and oily wastewater frequently has a pH of this level (Wenzlick & Siefert, 2020). The experiment of Chen et al. (2022) illustrated that when the pH was under 6, the Al_2O_3 membrane's zeta potential was positive, but when the pH was above 6, a negative surface charge was seen. While in the investigated pH range (2–10), the SiC-deposited membranes kept a negative surface charge (Chen et al., 2022). The same conclusion was found that as pH rose, the Al_2O_3 membrane's surface charge shifted toward the negative (Zhang et al., 2009) since the stronger electrostatic repulsion makes the negatively charged oil droplets less likely to clog the membrane surface. It could be predicted that the SiC-deposited membrane will have better performance compared with the Al_2O_3 membrane when dealing with negative nano-sized O/W emulsions.

The zeta potentials of the Al_2O_3 and SiC-deposited membranes were nearly equivalent at a pH of 10, but the water contact angle of the Al_2O_3 membrane (25°) was higher than that of the SiC-deposited membrane (0°) (Chen et al., 2022), so the former is less hydrophilic. Hence, the hydrophilicity of the membranes should also be considered during pH experiments in this study.

2.5.2 Surfactants

Oil droplets in O/W emulsions typically have a charge, either positively or negatively, depending on the type and properties of the stabilizing surfactants (Table 1) which means that membrane fouling is also thought to be significantly influenced by electrostatic interactions between oil droplets and a charged membrane surface.

Table 1. The zeta potential of the nano-sized O/W emulsions stabilized with different surfactants

Type	Oil(mg/L)	Surfactant	pH	Zeta potential (mV)	Reference
Nano-sized O/W emulsion	10,000	1000 mg/L Tween 80, 1000 mg/L Span 80	~5.8	~-38	(Wang et al., 2022)
Micron-sized O/W emulsion	50	50 mg/L CTAB	5.76	61.87	(Trinh et al., 2019)
Micron-sized O/W emulsion	50	50 mg/L SDS	5.50	-38.53	(Trinh et al., 2019)

In the currently available literatures, there is disagreement over whether electrostatic attraction or repulsion contributes to the reduction of ceramic membrane fouling related to the constant pressure filtration. Lu et al. (2015) found that when tested with O/W emulsions stabilized with a surfactant that had a charge opposite to that of the membrane, the TiO_2/ZrO_2 ceramic membranes showed less irreversible fouling and a higher rejection of dissolved organics, and the main explanations for the lower fouling due to the avoidance of pore blockage (a synergistic steric effect and a demulsification effect). In contrast, an opposite example related to the role of electrostatic interaction in UF of O/W emulsions was reported by Matos et al. (2016), when filtering an emulsion stabilized with an anionic surfactant, the negatively charged ZrO_2/TiO_2 ceramic membrane had a higher flux, and the reason could be that the electrostatic repulsion lessens fouling by preventing the development of a cake layer on the membrane surface, at the same time, when filtering an emulsion stabilized with a cationic surfactant, a lower flux was noticed.

There are two main reasons could explain the different phenomenon. Firstly, the disparities in the feed characteristics, such as oil droplet size, surfactant concentration,

and salinity, could account for the conflicting results on the impact of electrostatic interaction on membrane fouling (Chen et al., 2022). Secondly, in addition to the interaction between oil droplets and membrane surfaces, changing hydrodynamic conditions and solute concentrations close to the membrane also contribute to the observed fouling behavior since the mode of operation for these studies was constant pressure filtration (Miller et al., 2014).

However, the electrostatic repulsion is considered to lessen the fouling in the constant flux filtration, for example, Chen et al. (2022) found that the fouling of the SiC-deposited membrane was significantly lower than that of the Al_2O_3 membrane at a low concentration of negatively charged surfactant sodium dodecyl sulfate (33 mg L^{-1} SDS), and the higher irreversible fouling of the Al_2O_3 membrane was attributed to the absence of electrostatic repulsion between the membrane and oil droplets. SDS of 50 mg L^{-1} was selected in this study, so it should be observed that the SiC-deposited membrane has less fouling compared with the Al_2O_3 membrane when dealing with nano-sized O/W emulsions stabilized with Span 80 and SDS. The effects of nano-sized O/W emulsions stabilized by different surfactants would be further illustrated in Chapter 4.

2.5.3 Salinity

The stability of oil emulsions (Tambe & Sharma, 1993) as well as the membrane surface (Kwon et al., 2000) are both known to be impacted by salt, which would change the interactions between the oil and membrane and consequently the fouling behavior.

Tanudjaja et al. (2017) demonstrated that the presence of salt increased the likelihood of membrane fouling due to the changes in the density of the continuous phase as well as interfacial interaction energy between emulsion and membrane. Firstly, the density of the continuous phase increased along with the salt concentration, which in turn increased the density differential between the continuous and dispersed phases (Kwon

et al., 2000), and this increased the tendency of the oil droplets to rise toward the membrane. Secondly, as the concentration of salt increased, the charges on the membrane surface (Tanudjaja et al., 2017) and oil droplets (Elzo et al., 1998) would decrease. For instance, Tanudjaja et al. (2017) found that the Al_2O_3 membrane's surface potential (Malvern Zetasizer Nano ZS) became less negative with an increase in salt concentration, and the oil emulsion's zeta potential changed from negative to positive values at the same time. It was also demonstrated by the experiment of Onaizi (2022) that when the nanoemulsion was stabilized by the anionic Sodium dodecyl benzene sulfonate (SDBS) surfactant, the addition of Na^+ through the addition of NaCl would cause Na^+ to penetrate through the electric double layer to the droplet surface and neutralize the surfactant's counterions. A lower absolute zeta potential would result from this charge screening effect because it would weaken the electric field and consequently decrease the electrophoretic mobility of the emulsion droplets.

The strength of the interface or the integrity of the oil drops is significantly influenced by the oil−water interfacial tension. Dickhout et al. (2019) also used the interfacial tension to illustrate the effect of the salinity, for example, the interfacial tension of the oil-water interface in the presence of SDS (231 mg/L) decreased with increasing ionic strength as the negatively charged SDS head groups were screened by the positively charged sodium ions while more surfactant will adsorb to the droplet surfaces which thereby increased the surface charge density, overall, the electrostatic repulsion between droplets and droplets as well as the model surface decreases with increasing ionic strength. Meanwhile, droplets could adhere to the surface more firmly as the repulsive force between them weakened. Additionally, since the sodium ions also screen the electrostatic repulsion between the droplets, the colloidal stability of the emulsion may become less stable (Dickhout et al., 2018). The membrane fouling affected by the salinity also relates to the porosity of the cake layer since oil droplets strongly repel one another at low ionic strength, resulting in the formation of an open,

more permeable cake layer, while the screening of charge interactions results in a lower porosity and, consequently, a lower flux at higher ionic strengths (Dickhout et al., 2019).

When the NaCl concentration was less than or equal to 10 mM, the fouling of the SiC-deposited ceramic membrane was significantly lower than that of the Al_2O_3 ceramic membrane when treating the micron-sized O/W emulsions (Chen et al., 2022), and this shows that the fouling by oily wastewater with relatively low salinity was still influenced by the surface charge of the SiC-deposited membrane. High salt concentrations caused the counter-ions to screen the resulting surface charge of the droplet and the membrane surface while also allowing for more SDS adsorption on the oil-water interface (Dickhout et al., 2018). In this study, the low concentration of 1mM and 10mM NaCl were added with nano-sized O/W emulsions stabilized with SDS, so both membranes would suffer higher fouling when dealing with 10mM NaCl due to the compressed electrical double layer, meanwhile, the SiC-deposited membrane is predicted to have less fouling because of its negative charge surface and more hydrophilic surface.

Divalent cations like Ca^{2+}, which cause the diffusion double layer to compress more than monovalent ions, may hasten membrane fouling (Dickhout et al., 2017). Although the electrostatic repulsion weakened, the irreversible fouling of the SiC-deposited ceramic membrane was still lower than that of the Al_2O_3 ceramic membrane when treating micron-sized O/W emulsions (Chen et al., 2022). There are two reasons for why the membrane will suffer higher fouling when adding Ca^{2+} in the solutes. Firstly, Ca^{2+} and the sulfate group of SDS may form a complex because of SDS's interaction with divalent Ca^{2+} (Panpanit et al., 2000; Sammalkorpi et al., 2009). Fewer SDS molecules in the emulsion would increase the irreversible fouling of the membranes (Virga et al., 2020). Secondly, when Ca^{2+} is present in the emulsion, lower electrostatic charge of oil droplets and membranes is to be expected because of a compressed

electrostatic layer (Hong & Elimelech, 1997). Therefore, droplet coalescence on the membrane surface is encouraged, resulting in a less permeable cake layer (Tummons et al., 2017). In this study, 1mM $CaCl_2$ was added with 1mM NaCl to see whether the fouling of both membranes becomes more severe compared with 1mM NaCl experimental group.

2.6 Cleaning method

Membrane fouling with O/W emulsions restricts the use of membrane filtration in produced water treatment. To clean the membrane surface and restore water flow, various cleaning techniques are used. The techniques include chemical cleaning, mechanical cleaning (such as air back pulses, cleaning by ultrasound and membrane vibrations, and foulant removal by sponges sent through the interior of tubular membranes), and hydraulic cleaning (such as water flushes and water back flushes) (Tummons et al., 2020). The membranes must be disposed of and replaced when cleaning them is no longer sufficient to restore their functionality.

3. Materials and Methodology

3.1 Materials

3.1.1 The Al_2O_3 and SiC-deposited membranes

CoorsTek Industry (the Netherlands) provided single-channel tubular ceramic Al_2O_3 membranes with a pore size of 100 nm. The tubular Al_2O_3 membranes have an inner diameter of 6 mm, an outer diameter of 10 mm, and a length of 100 mm. Both the selective layer and the support layer are made of α-Al_2O_3. The membrane was manually sealed on both ends, and the total length of the sealed area was 2 cm. Therefore, the membrane's effective filtering area is 0.001507 m^2.

Low pressure chemical vapor deposition (LPCVD) was used to create the SiC-deposited membranes, with Al_2O_3 tubes serving as the support (CoorsTek Industry, the Nertherlands). The deposition time of 20 min was selected to obtain the SiC-deposited membrane. The characteristics of the membranes are listed in Table 2.

Table 2. Characteristics of the Al_2O_3 and SiC-deposited membranes

Properties	unit	Al_2O_3 membrane	SiC-deposited membrane
Pore size	nm	100	100
Clean water permeance	$Lm^{-2}h^{-1}bar^{-1}$	360	200
Length	cm	10	10
Sealed length	cm	2	2
Inner diameter	mm	6	6
Outer diameter	mm	10	10
Filtering area	m^2	0.001507	0.001507

3.1.2 Nano-sized O/W emulsions

Soybean oil (Signma-aldrich, Germany), Tween 80 (Signma-aldrich, Germany), Span 80 (Signma-aldrich, Germany), SDS (> 99%, Sigma-Aldrich), CTAB (Signma-aldrich, Germany) and demineralized water (pH= 5.8) were used to create nano-sized O/W emulsion with a concentration of 500 mg L^{-1}. With the addition of mixed surfactants (mass ratio of Span 80: Tween 80/SDS/CTAB≈1:1), high speed stirring at 2000 rpm with a magnetic stirrer for 1 day (L23, LABINCO, the Netherlands), followed by ultrasonication in a sonifier for 1 day (Branson Digital, USA), highly stable nano-sized O/W emulsions were prepared (Yan et al., 2019).

Since the typical oil concentration in oily wastewater ranges from 50 to 500 mg/L (Fakhru'l-Razi et al., 2009), a fresh emulsion with the oil concentration of 500 mg/L was created before each experiment using demineralized water. The concentration of Tween 80 and Span 80 was obtained at 50 mg/L for the synthesis of 500 mg/L nano-sized O/W emulsions, resulting in a mass ratio of soybean oil, Span 80, Tween 80, and demineralized water at 0.5: 0.05: 0.05: 1000 (Liu, 2022; Wang et al., 2022). In this study, the mass ratio of oil and surfactants is also selected as 10:1.

Ten different types of nano-sized O/W emulsions were prepared for the filtration experiment about pH, surfactant as well as salinity of the Al_2O_3 and SiC-deposited membranes respectively (Table 3).

Table 3. Ten kinds of nano-sized O/W emulsions for the Al_2O_3 (A1-A10) and SiC-deposited membranes (B1-B10) respectively

Solution	Oil concentration (mg/L)	Tween 80 (mg/L)	Span 80 (mg/L)	SDS (mg/L)	CTAB (mg/L)	NaCl (mM)	$CaCl_2$ (mM)	pH
A1, B1	500	0	50	50	0	0	0	4
A2, B2	500	0	50	50	0	0	0	5.8
A3, B3	500	0	50	50	0	0	0	8
A4, B4	500	0	50	50	0	0	0	10
A5, B5	500	50	50	0	0	0	0	5.8
A6, B6	500	0	50	50	0	0	0	5.8
A7, B7	500	0	50	0	50	0	0	5.8
A8, B8	500	0	50	50	0	1	0	5.8
A9, B9	500	0	50	50	0	10	0	5.8
A10, B10	500	0	50	50	0	1	1	5.8

3.2 Filtration Set-up

For constant flux experiments, a membrane filtration set-up with backwash was created (Figure 2). To reach the same water permeability, a fixed pressure of 5.4 bar was set for SiC membrane backwashing, and a fixed pressure of 3 bar was set for Al_2O_3 membrane backwashing based on their different water permeance. The backwashing vessel filled with demineralized water was connected to a compressed air system. A circulation pump (Van Wijk & Boersma) provided a constant crossflow velocity which was measured by a flow meter, while a feed pump (Grundfos, DDA) dosed the nano-sized O/W emulsion into the circulation loop and controlled the permeate flux. To track TMP changes, two high-precision pressure transducers (GS4200-USB, ESI, UK) were installed on either side of the membrane module. In case there was a discrepancy between the feed pump flow and the permeate flux, a digital balance was used to measure the permeate flux. Pressure, temperature, and flow were continuously recorded throughout the experiments at intervals of 30 s.

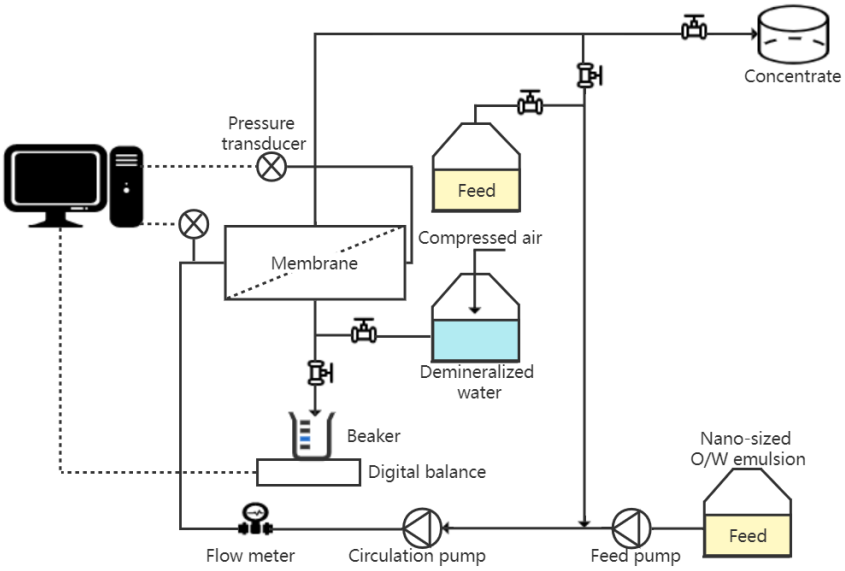

Figure 2. Schematic view of the constant flux crossflow filtration setup

3.3 Experiment procedure

The constant flux filtration setup described above was used to test the Al_2O_3 and SiC-deposited membranes separately to compare the membrane fouling resistance before and after deposition. In this study, the nano-sized O/W emulsion was used as a foulant.

A permeability test on demineralized water was the first step in every filtration experiment with TMP ranging between 0.2 bar and 0.7 bar due to the different intrinsic membrane resistance, and pure water fluxes were measured using demineralized water and the backwash tank. All experiments will be performed in duplicate, and temperature and pressure will be adjusted according to the value of the day because they will affect permeate flux. The system was then flushed with the feed stream before the filtration experiments began to remove air bubbles in the pipes. The cross flow velocities for the forward flush were maintained at 2 m/s, and the procedure took place for 2 minutes.

There were six cycles in each fouling experiment, and each cycle was made up of three phases in the following order: 1) Filtration of the nano-sized O/W emulsion for 20 minutes at a constant flux. 2) Remove the hydraulically reversible fouling by backwashing the membrane module with demineralized water at a fixed pressure of 5.4 bar or 3 bar for 30 s. 3) 15 seconds of forward flush with the feed at a crossflow speed of 2 m/s. The forward flush was used to purge the membrane to get rid of any leftover backwash liquids and replace the solution in the loop with fresh feed.

The setup for the experiments should be washed for 10 minutes with demi water at a cross flow velocities of 2 m/s after each filtration experiment to drain the concentrate water in the pipe. Next, the membrane was taken out and put into the bottle containing 0.1M NaOH solution for 1 hour at 65 ˚C hot water bath then put in the oven under 200℃ for 1 hour.

3.4 Data Analysis

Chemical oxygen demand (COD) of the samples was measured by a Hach spectrophotometer (DR 3900, US) with COD cuvettes (LCK 514 and LCK 314, Hach) (Marchese et al., 2000), while the oil concentration of the samples was measured by a UV/Vis spectrophotometer (GENESYS 10S UV-Vis, Thermo scientifical, US) at 275 nm (Zhou et al., 2010). A calibration curve of oil concentration versus COD refers to the drawing by Liu (2022), then the oil and COD rejection of the membranes were calculated by equation (1):

$$R = \left(1 - \frac{C_p}{C_f}\right) \times 100\% \quad (1)$$

R - the rejection
C_p - the oil (mg/L) or COD concentration (mg/L) in the permeate
C_f - the oil (mg/L) or COD concentration (mg/L) in the feed.

The TMP increased over time in the constant flux filtration experiment because oil droplets fouled the membrane. The membrane permeance was calculated as equation (2):

$$L = \frac{J}{TMP} \quad (2)$$

L - the membrane permeance,
J - the permeate flux (m/s),
TMP - the transmembrane pressure (Pa).

The membrane resistance was calculated as shown in equation (3)(4)(5)(6):

$$J = \frac{\Delta P}{\mu(R_m + R_r + R_{ir})} \quad (3)$$

$$R_m = \frac{\Delta P_0}{\mu J} \quad (4)$$

$$R_{ir} = \frac{\Delta P_b}{\mu J} - R_m \quad (5)$$

$$R_r = \frac{\Delta P_e}{\mu J} - \frac{\Delta P_b}{\mu J} \quad (6)$$

ΔP - the transmembrane pressure,
ΔP_0 - the TMP of clean membrane at the start of the experiment,
ΔP_e - the TMP of membrane at the end of the experiment,
ΔP_b - the TMP of membrane after the backwash,
μ - the viscosity of the permeate (Pa·s),
R_m - the intrinsic membrane resistance (m^{-1}),
R_r - the hydraulically reversible resistance (m^{-1}),
R_{ir} - the irreversible unphysical removable resistance (m^{-1}).

4. Results and Discussion

4.1 Oil rejection

In all nano-sized O/W emulsion separation experiments based on the adjustment of pH, surfactants and salinity, the oil rejection was very high (Fig. S 1). For oil rejection calculated by the absorbance data, the oil rejection of the Al_2O_3 membrane was higher than 96.8%, and the oil rejection of the SiC-deposited membrane was higher than 97.9%. For oil rejection calculated by the COD data, the oil rejection of the Al_2O_3 membrane was higher than 95.6%, and the oil rejection of the SiC-deposited membrane was higher than 96.6%. It could be illustrated by the formation of cake filtration (Kirschner et al., 2019) as well as hydrophilic membrane surfaces.

In addition, no obvious variations in oil rejection were observed for nano-sized O/W emulsions stabilized with different pH, surfactants, and salinity selected in this study (Fig. S 1).

4.2 pH

To investigate the effect of pH on the fouling of Al_2O_3 and SiC-deposited ceramic membranes, three different pH values (pH 4, pH 5.8 and pH 8) were selected in this

study. In all cases, the fouling was more in the Al_2O_3 membrane than in the SiC-deposited membrane and the fouling on both membranes decreased with a rise in pH. This could be attributed to the fact that, the membrane surface charge becomes more negative when the pH rises (Zhang et al., 2009).

Specifically, the zeta potential of the Al_2O_3 membrane was positive when the pH was less than 6, and it was negative when the pH was greater than 6, while the SiC-deposited membranes maintained a negative surface charge across the tested pH range (2–10) (Chen et al., 2022). Therefore, when pH was less than 6, the SiC-deposited membrane had greater electrostatic repulsion force on negatively charged nano-sized O/W emulsions stabilized with SDS, hence possessed less fouling. The zeta potentials of both membranes were quite similar at higher pH (Chen et al., 2022), but the SiC-deposited membrane had the greater hydrophilicity (He & Vidic, 2016; Hofs et al., 2011), so it behaved better than the Al_2O_3 membrane.

The normalized TMP comparison of two membranes is shown in Figure 3. It could be observed that the normalized TMP of the Al_2O_3 membrane was still higher than that of the SiC-deposited membrane with increasing time and the increase in the normalized TMP of both membranes became slower with the increase of pH. It indicated that both membranes had less foulling under the higher pH condition and the SiC-deposited membrane behaved better under all pH cases.

From the normalized permeability curve for two membranes (Figure 4), it could be seen that the SiC-deposited membrane always had the higher permeability than that of the Al_2O_3 membrane and the slope of the normalized permeability curves for both membranes became slower with the increase of pH. It verified that SiC-deposited membrane had less fouling under all pH conditions.

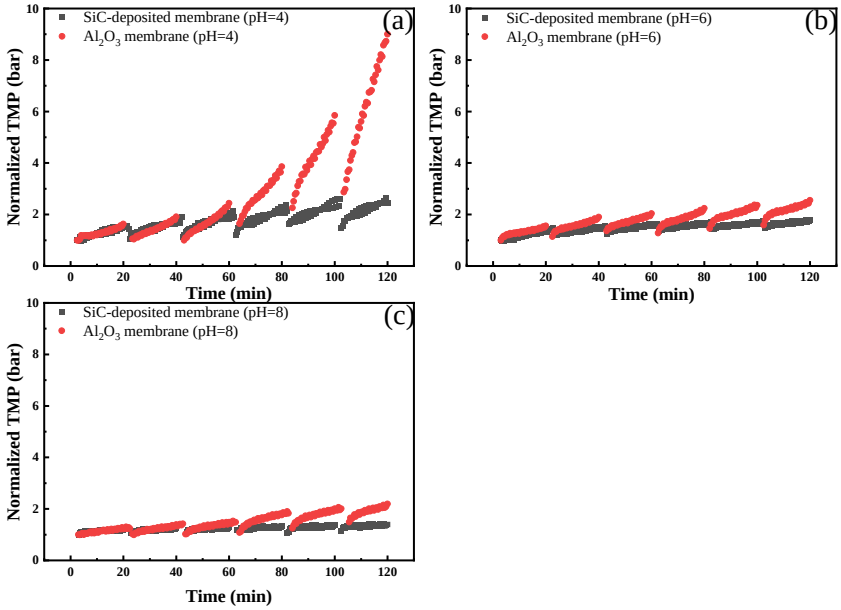

Figure 3. Comparison of the normalized TMP between the SiC-deposited membrane and Al_2O_3 membrane with different pH filtering 500 mg/L nano-sized O/W emulsions stabilized with Span 80 and SDS: (a) pH = 4, (b) pH = 6, and (c) pH = 8.

The irreversible fouling and reversible fouling of the Al_2O_3 membrane were much higher than that of the SiC-deposited membrane under all the pH conditions (Figure 5). For the SiC-deposited membrane, the reversible fouling dominated the fouling. It could be possibly illustrated by the cake filtration and the reversible fouling could be removed from the hydraulic washing.

The comparison of the normalized TMP curve and the normalized fouling resistance curve of the same membrane under different pH conditions could be seen in Fig. S 2.

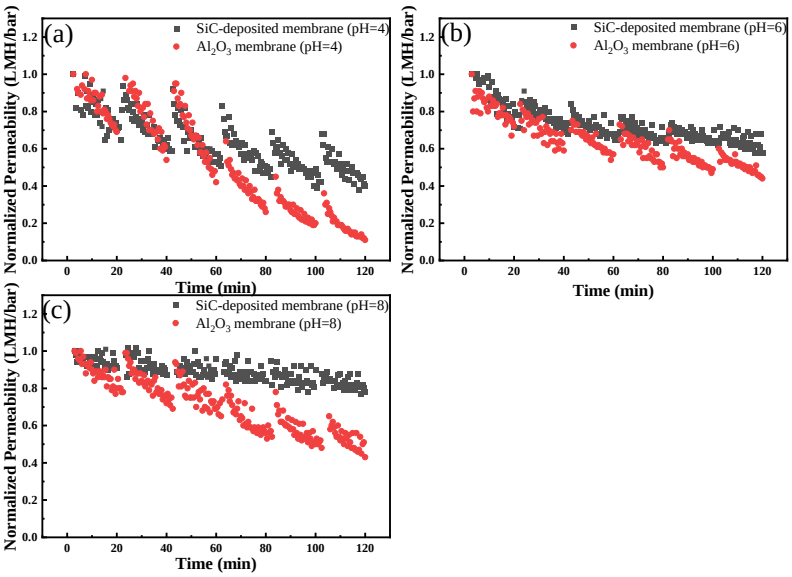

Figure 4. Comparison of the mormalized permeability between the SiC-deposited membrane and Al_2O_3 membrane with different pH filtering 500 mg/L nano-sized O/W emulsions stabilized with Span 80 and SDS: (a) pH = 4, (b) pH = 6, and (c) pH = 8.

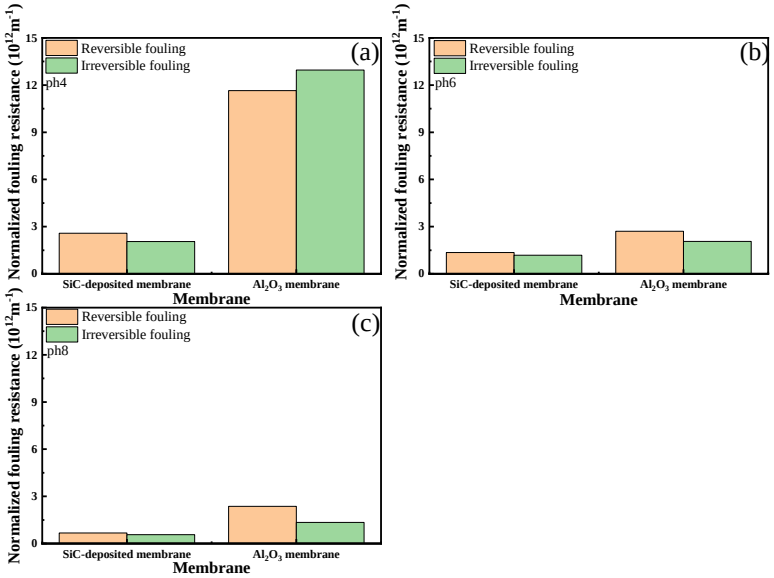

Figure 5. Comparison of the normalized fouling resistance between the SiC-deposited membrane and Al_2O_3 membrane with different pH filtering 500 mg/L nano-sized O/W emulsions stabilized with Span 80 and SDS: (a) pH = 4, (b) pH = 6, and (c) pH = 8.

4.3 Surfactants

Span 80, SDS, CTAB and Tween 80 were used to investigate the effect of the different surfactants on fouling of the Al_2O_3 membrane and SiC-deposited membrane under pH 6. The droplet size of oil was not changed with the adding of surfactants in this study (Table. S 2). Overall, when comparing two membranes, the Al_2O_3 membrane had less fouling dealing with the nano-sized O/W emulsions stabilized with Span 80/CTAB, while the SiC-deposited membrane had less fouling dealing with the nano-sized O/W emulsions stabilized with Span 80/SDS and Span 80/Tween 80.

This phenomenon could be explained by the electrostatic repulsion and attraction between the membrane and oil droplets, the degree of the hydrophilicity of the membrane surface as well as the effect of the surfactant adsorption. At pH 6, the Al_2O_3 membrane is positively charged, while the SiC-deposited membrane is negatively charged (Chen et al., 2022). The nano-sized O/W emulsions stabilized with Span 80/CTAB are positively charged, while the nano-sized O/W emulsions stabilized with Span80/Tween 80 are negatively charged (Trinh et al., 2019; Wang et al., 2022). So when the membrane and nano-sized O/W emulsions stabilized with surfactants have the same type of the charge, the repulsion force is greater which causes less fouling. Moreover, the adsorption of SDS on the positively charged Al_2O_3 membrane was also consider when dealing with the Span 80/SDS-stabilized nanoemulsions, as the surface charge of the Al_2O_3 membrane may be reversed from positive to negative (Chen et al., 2022), so both membranes had electrostatic repulsion to negatively charged Span 80/SDS-stabilized nanoemulsions, but the SiC-deposited membrane had less fouling under this case due to more hydrophilic surface.

From the normalized TMP curve for both membrane dealing with nano-sized O/W emulsions stabilized with different surfactants, it could be found that the SiC-deposited

membrane had less normalized TMP compared with the Al_2O_3 membrane when dealing with nano-sized O/W emulsions stabilized with Span 80/SDS or Span 80/Tween 80, while the Al_2O_3 membrane had less normalized TMP under the situation of Span 80/CTAB. The reasons were first illustrated by the electrostatic repulsion and electrostatic attraction as mentioned before and this effect was supported by the results of the zeta potential of nano-sized O/W emulsions stabilized with different surfactants (Table. S 1). As the mean zeta potential of Span 80/CTAB-stabilized nanoemulsions at pH 6 is 62.67 mV which means Span 80/CTAB-stabilized nanoemulsions are positively charged, so positively charged Al_2O_3 membranes would have more electrostatic repulsion to Span 80/CTAB-stabilized nanoemulsions compared with the negatively charged SiC-deposited membrane. While the mean zeta potential of Span 80/Tween 80-stabilized nanoemulsions at pH 6 is -21.3 mV, hence negatively charged SiC-deposited would have more electrostatic repulsion compared with positively charged Al_2O_3 membranes. The SiC-deposited membrane had lower normalized TMP when dealing with Span 80/SDS-stabilized nanoemulsions compared with the Al_2O_3 membrane could be further illustrated by the effect of the SDS adsorption and the degree of the hydrophilicity of the membrane surface as mentioned above.

However, the Al_2O_3 membrane had higher TMP dealing with nano-sized O/W emulsions stabilized with Span 80/Tween 80 than dealing with nano-sized O/W emulsions stabilized with Span 80/SDS. It could be considered from the aspect of SDS adsorption. Based on the adsorption model proposed by Gu and Zhu (1990), the first layer is preferably formed by the head groups of surfactant monomers adhering to the hydrophilic membrane surfaces, then a second layer is adsorbed on top of the previous one. The negatively charged and hydrophilic head of the SDS was attached to the positively charged Al_2O_3 membrane surface because of the electrostatic attraction as a monolayer, then a new monolayer was attached to this covered monolayer, and the hydrophilic head and negatively charged of SDS was oriented towards the solution

phase due to hydrophobic interactions leading to membrane charge inversion (Chen et al., 2022). There was the electrostatic repulison between the Al_2O_3 membrane and Span 80/SDS-stabilized nanoemulsions, while there was the electrostatic attraction between the Al_2O_3 membrane and Span 80/Tween 80-stabilized nanoemulsions, hence the former condition had less fouling. While for the SiC-deposited membrane, electrostatic repulsion effect is dominant, and Span 80/SDS-stabilized nanoemulsions are more negatively charged compared with Span 80/Tween 80-stabilized nanoemulsions (Table. S 1), so negatively charged SiC-deposited membrane had lower TMP under the situation of Span 80/SDS rather than Span 80/Tween 80.

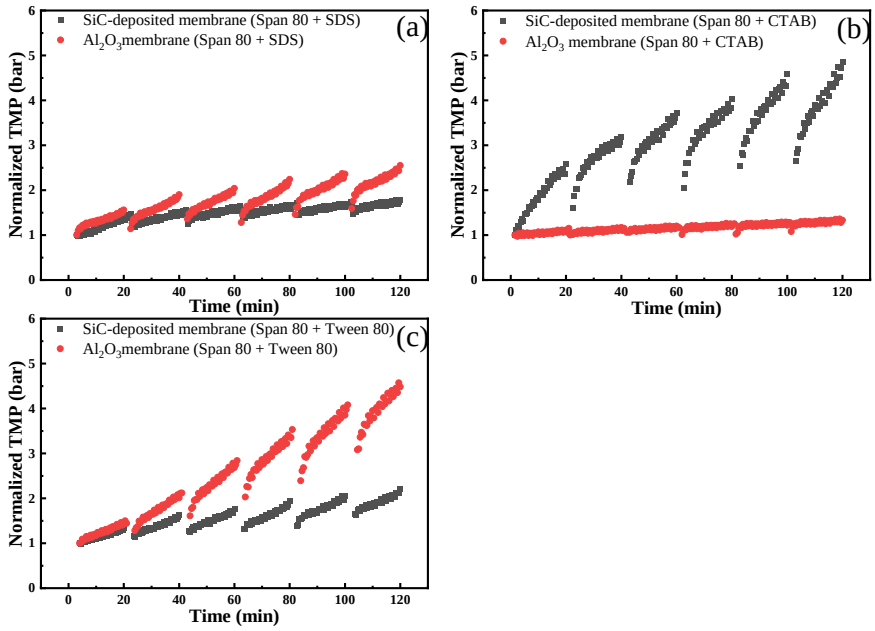

Figure 6. Comparison of the normalized TMP between the SiC-deposited membrane and Al_2O_3 membrane filtering 500 mg/L nano-sized O/W emulsions stabilized with different surfactants: (a) Span 80/SDS, (b) Span 80/CTAB, and (c) Span 80/Tween 80.

The normalized permeability curve verified the conclusion acquired from the normalized TMP curve (Figure 7). It could be observed that the SiC-deposited membrane had higher normalized permeability compared with the Al_2O_3 membrane

when dealing with nano-sized O/W emulsions stabilized with Span 80/SDS or Span 80/Tween 80, while the Al_2O_3 membrane had higher normalized permeability under the situation of Span 80/CTAB. This phenomenon could be ascribed to the effect of the electrostatic repulsion supported by the zeta potential results of nano-sized O/W emulsions stabilized with different surfactants (Table. S 1). Moreover, the Al_2O_3 membrane had lower permeability dealing with nano-sized O/W emulsions stabilized with Span 80/Tween 80 than dealing with nano-sized O/W emulsions stabilized with Span 80/SDS. The reasons could be explained by the SDS adsorption leading to the membrane surface charge inversion.

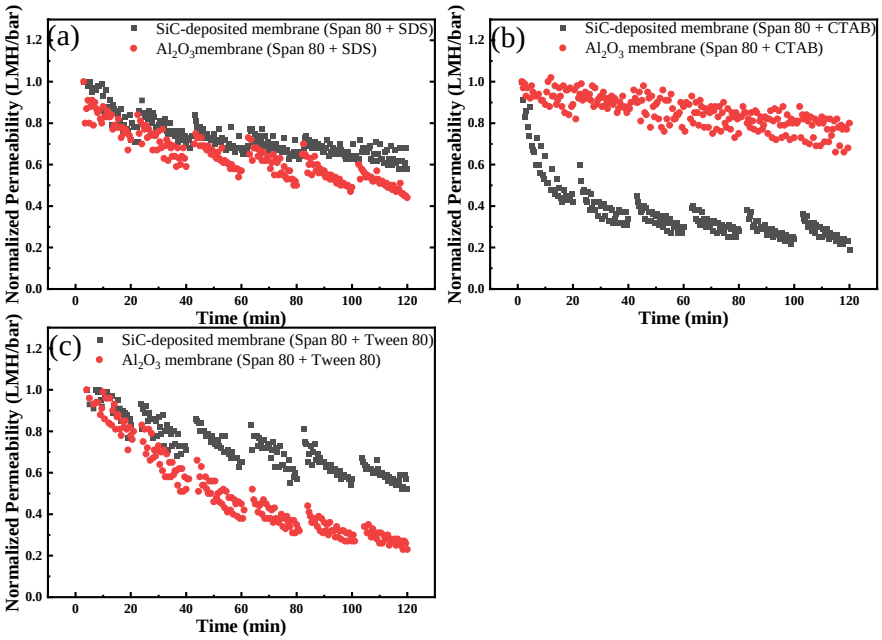

Figure 7. Comparison of the normalized permeability between the SiC-deposited membrane and Al_2O_3 membrane filtering 500 mg/L nano-sized O/W emulsions stabilized with different surfactants: (a) Span 80/SDS, (b) Span 80/CTAB, and (c) Span 80/Tween 80.

The Al_2O_3 membrane had less fouling resistance when dealing with the nano-sized O/W emulsions stabilized with Span 80/CTAB, while the SiC-deposited membrane had less fouling resistance when dealing with the nano-sized O/W emulsions stabilized with

Span 80/SDS or Span 80/Tween 80. Although SiC-deposited had more fouling compared with the Al_2O_3 membrane when dealing with nano-sized O/W emulsions stabilized with Span 80/CTAB, the reversible fouling was dominant for the SiC-deposited membrane under this situation which may be caused by the cake filtration and the reversible fouling could be removed from the hydraulic washing.

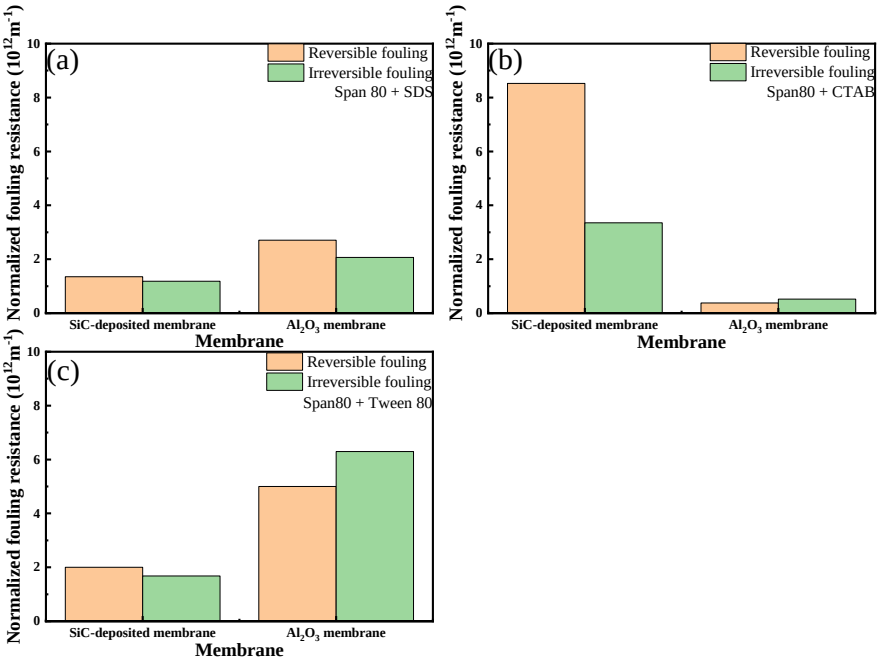

Figure 8. Comparison of the normalized fouling resistance between the SiC-deposited membrane and Al_2O_3 membrane filtering 500 mg/L nano-sized O/W emulsions stabilized with different surfactants: (a) Span 80/SDS, (b) Span 80/CTAB, and (c) Span 80/Tween 80.

The comparison of the normalized TMP curve and the normalized fouling resistance curve of the same membrane under different surfactant conditions could be seen in Fig. S 3.

4.4 Salinity

The effect of the salinity on both membranes fouling was conducted by adding 1mM NaCl, 10mM NaCl and 1mM NaCl/1mM $CaCl_2$. The nano-sized O/W emulsions were

stabilized with SDS/ Span 80 with pH of 5.8. Both membranes experienced higher fouling with the increasing concentration of NaCl from 1mM to 10mM, and the SiC-deposited membrane had less fouling compared with the Al_2O_3 membrane.

It could be illustrated by the lower absolute zeta potential of the membrane surface and the nano-sized O/W emulsions (Elzo et al., 1998; Onaizi, 2022; Tanudjaja et al., 2017) which results from the charge screening effect and the decrease of the oil−water interfacial tension (Dickhout et al., 2019).

Specifically, the charge screening effect and the less oil-water interfacial tension let the electrostatic repulsion between nano-sized O/W emulsions and nano-sized O/W emulsions as well as the membrane surface decrease with increasing salinity. Another possible reason could be the change of the porosity of the cake layer as a less porosity cake layer forms at higher salinity leading to a lower flux (Dickhout et al., 2019).

When comparing the fouling of both membranes under the condition of 1mM NaCl and 1mM NaCl/1mM $CaCl_2$, both membranes experienced more severe fouling when adding Ca^{2+} as the divalent cations compresses the diffusion double layer more than the monovalent cations like Na^+ (Dickhout et al., 2017), while the SiC-deposited membrane has less fouling due to its negative surface charge effect and the more hydrophilic surface.

The normalized TMP curve (Figure 9) and the normalized permeability curve (Figure 10) for both membranes under different salinity conditions verified the conclusion mentioned above. The SiC-deposited membrane had less normalized TMP and higher permeability in all salinity cases compared with the Al_2O_3 membrane, and both membranes experienced higher TMP and less permeability when adding more Na^+ or introducing Ca^{2+}. The addition of Ca^{2+} caused more severe fouling when compared with the addition of Na^+.

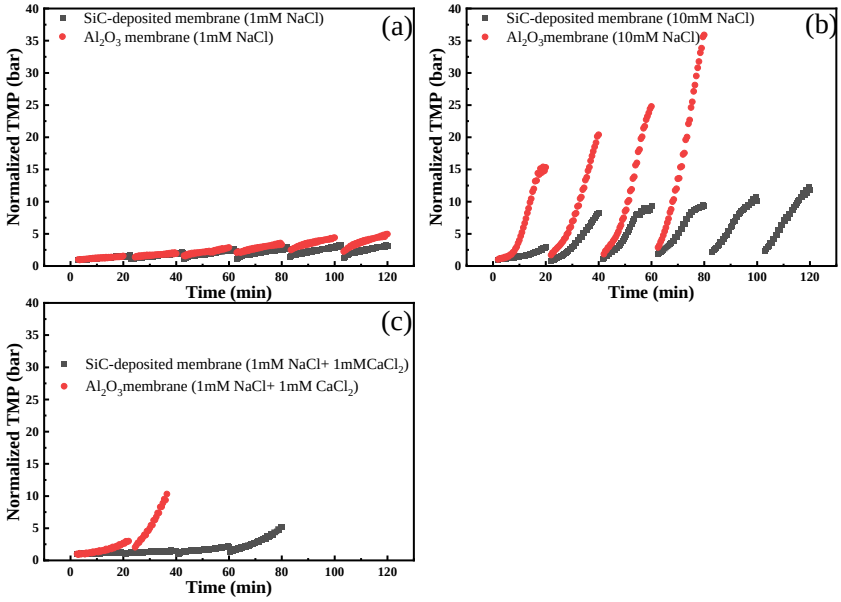

Figure 9. Comparison of the normalized TMP between the SiC-deposited membrane and Al_2O_3 membrane with different salinity filtering 500 mg/L nano-sized O/W emulsions stabilized with Span 80 and SDS: (a) 1 mM NaCl, (b) 10 mM NaCl, and (c) 1 mM NaCl + 1 mM $CaCl_2$.

The irreversible fouling resistance of the Al_2O_3 membrane was much higher than that of the SiC-deposited membrane under all the salinity conditions, hence the SiC-deposited has the better performance. Moreover, the reversible fouling dominated the fouling on the SiC-deposited membrane under different salinity conditions due to the cake layer formation and could be further removed by hydraulic washing.

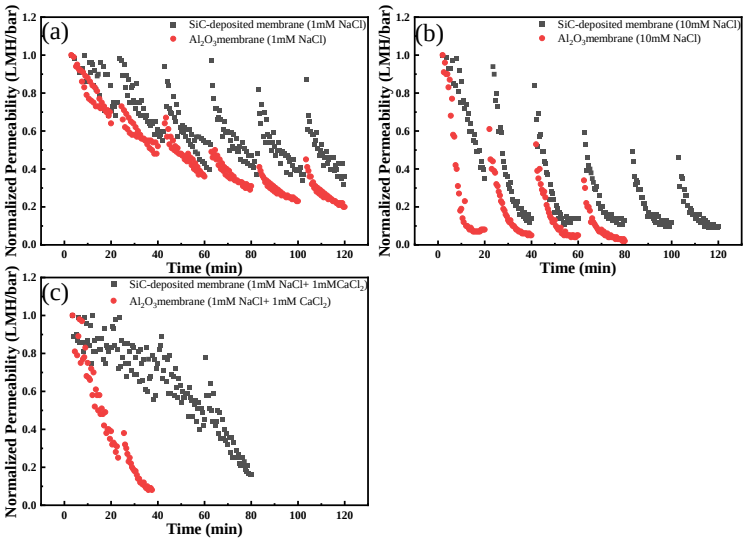

Figure 10. Comparison of the normalized permeability between the SiC-deposited membrane and Al_2O_3 membrane with different salinity filtering 500 mg/L nano-sized O/W emulsions stabilized with Span 80 and SDS: (a) 1 mM NaCl, (b) 10 mM NaCl, and (c) 1 mM NaCl + 1 mM $CaCl_2$.

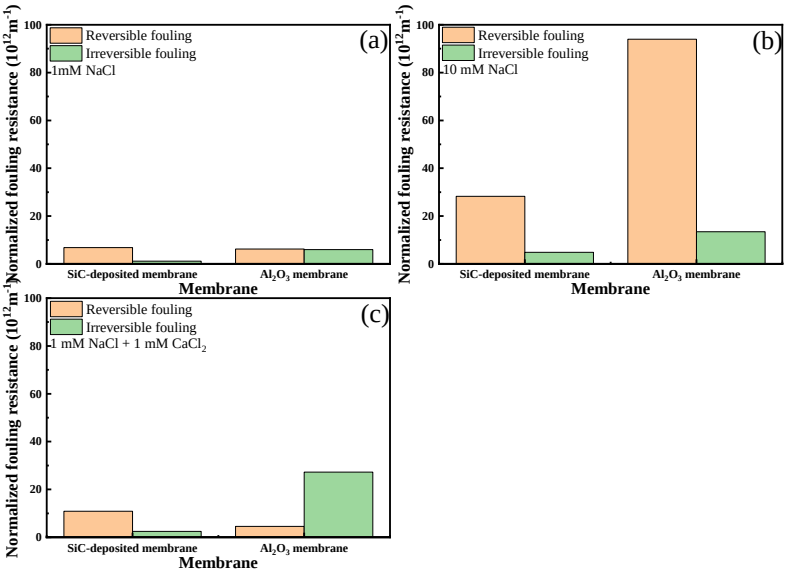

Figure 11. Comparison of the normalized fouling resistance between the SiC-deposited membrane and Al_2O_3 membrane with different salinity filtering 500 mg/L nano-sized O/W emulsions stabilized with Span 80 and SDS: (a) 1 mM NaCl, (b) 10 mM NaCl, and (c) 1 mM NaCl + 1 mM $CaCl_2$.

The comparison of the normalized TMP curve and the normalized fouling resistance curve of the same membrane under different salinity conditions could be seen in Fig. S 4.

5. Conclusion

The performance of Al_2O_3 and SiC-deposited ceramic membranes was systematically compared during constant flux UF of nano-sized O/W emulsions with six filtration cycles. This study aim to investigate the effects of different pH, surfactants as well as salinity on the fouling of both ceramic membranes. The hypothesis to the research questions were verified through the experiments, and the conclusions were summarized as follows:

1) Fouling on both membranes decreased with a rise in pH due to more negative surface charge and higher electrostatic repulsion between the membrane and the nano-sized O/W emulsions. The fouling on the SiC-deposited membrane was always less than that of the Al_2O_3 membrane during the whole pH range because of the negatively charged and more hydraulic surface.

2) The SiC-deposited membrane had less fouling when dealing with nano-sized O/W emulsions stabilized with Span 80/SDS, as well as Span 80/Tween 80, while the Al_2O_3 membrane had less fouling when dealing with nano-sized O/W emulsions stabilized with Span 80/CTAB, and these could be illustrated by the electrostatic repulsion and attraction, the degree of the membrane surface hydrophilicity and the adsorption of the surfactants. When comparing the conditions under Span 80/SDS and Span 80/Tween 80, both membranes had less fouling with Span 80/SDS, as the Al_2O_3 membranes may had the surface charge inversion due to the SDS adsorption.

3) Both membranes experienced severe fouling when increasing the concentration of NaCl from 1mM to 10mM due to the charge screening effect and the less oil−water

interfacial tension. The addition of Ca^{2+} caused more severe fouling for both membranes when compared with the addition of Na^{+} as the divalent cations due to the more compression of the diffusion double layer compared to monovalent ions. The SiC-deposited membrane had less fouling compared with the Al_2O_3 membrane under different salinity conditions which attributed to the negatively charged and more hydrophilic surface.

Reference

Abadi, S. R. H., Sebzari, M. R., Hemati, M., Rekabdar, F., & Mohammadi, T. (2011). Ceramic membrane performance in microfiltration of oily wastewater. *Desalination*, *265*(1-3), 222-228.

Barredo-Damas, S., Alcaina-Miranda, M. I., Bes-Piá, A., Iborra-Clar, M. I., Iborra-Clar, A., & Mendoza-Roca, J. A. (2010). Ceramic membrane behavior in textile wastewater ultrafiltration. *Desalination*, *250*(2), 623-628. https://doi.org/https://doi.org/10.1016/j.desal.2009.09.037

Chen, H., Jia, X., Wei, M., & Wang, Y. (2017). Ceramic tubular nanofiltration membranes with tunable performances by atomic layer deposition and calcination. *Journal of Membrane Science*, *528*, 95-102. https://doi.org/https://doi.org/10.1016/j.memsci.2017.01.020

Chen, M., Heijman, S. G. J., Luiten-Olieman, M. W. J., & Rietveld, L. C. (2022). Oil-in-water emulsion separation: Fouling of alumina membranes with and without a silicon carbide deposition in constant flux filtration mode. *Water Research*, *216*, 118267. https://doi.org/https://doi.org/10.1016/j.watres.2022.118267

Chen, M., Shang, R., Sberna, P. M., Luiten-Olieman, M. W., Rietveld, L. C., & Heijman, S. G. (2020). Highly permeable silicon carbide-alumina ultrafiltration membranes for oil-in-water filtration produced with low-pressure chemical vapor deposition. *Separation and Purification Technology*, *253*, 117496.

Chen, M., Zhu, L., Dong, Y., Li, L., & Liu, J. (2016). Waste-to-Resource Strategy To Fabricate Highly Porous Whisker-Structured Mullite Ceramic Membrane for Simulated Oil-in-Water Emulsion Wastewater Treatment. *ACS Sustainable Chemistry & Engineering*, *4*(4), 2098-2106. https://doi.org/10.1021/acssuschemeng.5b01519

Chen, W., Su, Y., Zheng, L., Wang, L., & Jiang, Z. (2009). The improved oil/water separation performance of cellulose acetate-graft-polyacrylonitrile membranes. *Journal of Membrane Science*, *337*(1-2), 98-105. https://doi.org/10.1016/j.memsci.2009.03.029

Chen, Y., & Liu, Q. (2020). Progress and Prospects in Membrane Technology for Oil/Water Separation. In *Multidisciplinary Advances in Efficient Separation Processes* (Vol. 1348, pp. 73-87). American Chemical Society. https://doi.org/doi:10.1021/bk-2020-1348.ch003

10.1021/bk-2020-1348.ch003

Committee, A. S. o. P. P. o. t. M. P. (2008). Microfiltration and ultrafiltration membranes for drinking water. *Journal-American Water Works Association*, *100*(12), 84-97.

Cui, J., Zhang, X., Liu, H., Liu, S., & Yeung, K. L. (2008). Preparation and application of zeolite/ceramic microfiltration membranes for treatment of oil contaminated water. *Journal of Membrane Science*, *325*(1), 420-426. https://doi.org/https://doi.org/10.1016/j.memsci.2008.08.015

Dickhout, J. M., Kleijn, J. M., Lammertink, R. G., & De Vos, W. M. (2018). Adhesion of emulsified oil droplets to hydrophilic and hydrophobic surfaces–effect of surfactant charge, surfactant concentration and ionic strength. *Soft Matter*, *14*(26), 5452-5460.

Dickhout, J. M., Lammertink, R. G., & de Vos, W. M. (2019). Membrane filtration of anionic surfactant stabilized emulsions: effect of ionic strength on fouling and droplet adhesion. *Colloids and Interfaces*, *3*(1), 9.

Dickhout, J. M., Moreno, J., Biesheuvel, P. M., Boels, L., Lammertink, R. G. H., & de Vos, W. M. (2017). Produced water treatment by membranes: A review from a colloidal perspective. *Journal of Colloid and Interface Science*, *487*, 523-534. https://doi.org/https://doi.org/10.1016/j.jcis.2016.10.013

Ding, X., Fan, Y., & Xu, N. (2006). A new route for the fabrication of TiO2 ultrafiltration membranes with suspension derived from a wet chemical synthesis. *Journal of Membrane Science*, *270*(1), 179-186. https://doi.org/https://doi.org/10.1016/j.memsci.2005.07.003

Ebrahimi, M., Ashaghi, K. S., Engel, L., Willershausen, D., Mund, P., Bolduan, P., & Czermak, P. (2009). Characterization and application of different ceramic membranes for the oil-field produced water treatment. *Desalination*, *245*(1), 533-540. https://doi.org/https://doi.org/10.1016/j.desal.2009.02.017

Ebrahimi, M., Willershausen, D., Ashaghi, K. S., Engel, L., Placido, L., Mund, P., Bolduan, P., & Czermak, P. (2010). Investigations on the use of different ceramic membranes for efficient oil-field produced water treatment. *Desalination*, *250*(3), 991-996. https://doi.org/10.1016/j.desal.2009.09.088

Elzo, D., Huisman, I., Middelink, E., & Gekas, V. (1998). Charge effects on inorganic membrane performance in a cross-flow microfiltration process. *Colloids and Surfaces A: Physicochemical and Engineering Aspects*, *138*(2), 145-159. https://doi.org/https://doi.org/10.1016/S0927-7757(96)03957-X

Fakhru'l-Razi, A., Pendashteh, A., Abdullah, L. C., Biak, D. R. A., Madaeni, S. S., & Abidin, Z. Z. (2009). Review of technologies for oil and gas produced water treatment. *Journal of hazardous materials*, *170*(2), 530-551. https://doi.org/https://doi.org/10.1016/j.jhazmat.2009.05.044

Gu, T., & Zhu, B.-Y. (1990). The S-type isotherm equation for adsorption of nonionic surfactants at the silica gel—water interface. *Colloids and Surfaces*, *44*, 81-87. https://doi.org/https://doi.org/10.1016/0166-6622(90)80189-B

He, C., & Vidic, R. D. (2016). Application of microfiltration for the treatment of Marcellus Shale flowback water: Influence of floc breakage on membrane

fouling. *Journal of Membrane Science*, *510*, 348-354. https://doi.org/https://doi.org/10.1016/j.memsci.2016.03.023

Hermia, J. (1982). Constant pressure blocking filtration laws: application to power-law non-Newtonian fluids.

Hofs, B., Ogier, J., Vries, D., Beerendonk, E. F., & Cornelissen, E. R. (2011). Comparison of ceramic and polymeric membrane permeability and fouling using surface water. *Separation and Purification Technology*, *79*(3), 365-374. https://doi.org/https://doi.org/10.1016/j.seppur.2011.03.025

Hong, S., & Elimelech, M. (1997). Chemical and physical aspects of natural organic matter (NOM) fouling of nanofiltration membranes. *Journal of Membrane Science*, *132*(2), 159-181. https://doi.org/https://doi.org/10.1016/S0376-7388(97)00060-4

Hu, L., Gao, S., Ding, X., Wang, D., Jiang, J., Jin, J., & Jiang, L. (2015). Photothermal-Responsive Single-Walled Carbon Nanotube-Based Ultrathin Membranes for On/Off Switchable Separation of Oil-in-Water Nanoemulsions. *ACS Nano*, *9*(5), 4835-4842. https://doi.org/10.1021/nn5062854

Hu, M.-X., Niu, H.-M., Chen, X.-L., & Zhan, H.-B. (2019). Natural cellulose microfiltration membranes for oil/water nanoemulsions separation. *Colloids and Surfaces A: Physicochemical and Engineering Aspects*, *564*, 142-151. https://doi.org/https://doi.org/10.1016/j.colsurfa.2018.12.045

Hua, F. L., Tsang, Y. F., Wang, Y. J., Chan, S. Y., Chua, H., & Sin, S. N. (2007). Performance study of ceramic microfiltration membrane for oily wastewater treatment. *Chemical Engineering Journal*, *128*(2), 169-175. https://doi.org/https://doi.org/10.1016/j.cej.2006.10.017

Janknecht, P., Lopes, A. D., & Mendes, A. M. (2004). Removal of Industrial Cutting Oil from Oil Emulsions by Polymeric Ultra- and Microfiltration Membranes. *Environmental Science & Technology*, *38*(18), 4878-4883. https://doi.org/10.1021/es0348243

Kirschner, A. Y., Cheng, Y.-H., Paul, D. R., Field, R. W., & Freeman, B. D. (2019). Fouling mechanisms in constant flux crossflow ultrafiltration. *Journal of Membrane Science*, *574*, 65-75. https://doi.org/https://doi.org/10.1016/j.memsci.2018.12.001

Kwon, D. Y., Vigneswaran, S., Fane, A. G., & Aim, R. B. (2000). Experimental determination of critical flux in cross-flow microfiltration. *Separation and Purification Technology*, *19*(3), 169-181. https://doi.org/https://doi.org/10.1016/S1383-5866(99)00088-X

Li, D., Huang, X., Huang, Y., Yuan, J., Huang, D., Cheng, G. J., Zhang, L., & Chang, C. (2019). Additive Printed All-Cellulose Membranes with Hierarchical Structure for Highly Efficient Separation of Oil/Water Nanoemulsions. *ACS Applied Materials & Interfaces*, *11*(47), 44375-44382. https://doi.org/10.1021/acsami.9b16647

Liu, H. (2022). *Performance and membrane fouling of alumina UF membranes in treating nano-sized oil-water emulsions*

Lu, D., Zhang, T., & Ma, J. (2015). Ceramic Membrane Fouling during Ultrafiltration of Oil/Water Emulsions: Roles Played by Stabilization Surfactants of Oil Droplets. *Environmental Science & Technology*, *49*(7), 4235-4244. https://doi.org/10.1021/es505572y

Marchese, J., Ochoa, N. A., Pagliero, C., & Almandoz, C. (2000). Pilot-scale ultrafiltration of an emulsified oil wastewater. *Environmental Science & Technology*, *34*(14), 2990-2996.

Matos, M., Gutiérrez, G., Lobo, A., Coca, J., Pazos, C., & Benito, J. M. (2016). Surfactant effect on the ultrafiltration of oil-in-water emulsions using ceramic membranes. *Journal of Membrane Science*, *520*, 749-759. https://doi.org/https://doi.org/10.1016/j.memsci.2016.08.037

Miller, D. J., Kasemset, S., Wang, L., Paul, D. R., & Freeman, B. D. (2014). Constant flux crossflow filtration evaluation of surface-modified fouling-resistant membranes. *Journal of Membrane Science*, *452*, 171-183. https://doi.org/https://doi.org/10.1016/j.memsci.2013.10.037

Mohammadi, T., Kazemimoghadam, M., & Saadabadi, M. (2003). Modeling of membrane fouling and flux decline in reverse osmosis during separation of oil in water emulsions. *Desalination*, *157*(1), 369-375. https://doi.org/https://doi.org/10.1016/S0011-9164(03)00419-3

Mulder, M., & Mulder, J. (1996). *Basic principles of membrane technology*. Springer science & business media.

Onaizi, S. A. (2022). Effect of salinity on the characteristics, pH-triggered demulsification and rheology of crude oil/water nanoemulsions. *Separation and Purification Technology*, *281*, 119956.

Panpanit, S., Visvanathan, C., & Muttamara, S. (2000). Separation of oil–water emulsion from car washes. *Water Science and Technology*, *41*(10-11), 109-116. https://doi.org/10.2166/wst.2000.0620

Pugazhenthi, G., Sachan, S., Kishore, N., & Kumar, A. (2005). Separation of chromium (VI) using modified ultrafiltration charged carbon membrane and its mathematical modeling. *Journal of Membrane Science*, *254*(1-2), 229-239.

Sammalkorpi, M., Karttunen, M., & Haataja, M. (2009). Ionic Surfactant Aggregates in Saline Solutions: Sodium Dodecyl Sulfate (SDS) in the Presence of Excess Sodium Chloride (NaCl) or Calcium Chloride (CaCl2). *The Journal of Physical Chemistry B*, *113*(17), 5863-5870. https://doi.org/10.1021/jp901228v

Stewart, M. (2009). *Oil Treating Systems. In Emulsions and Oil Treating Equipment*.

Tambe, D. E., & Sharma, M. M. (1993). Factors Controlling the Stability of Colloid-Stabilized Emulsions: I. An Experimental Investigation. *Journal of Colloid and*

Interface Science, *157*(1), 244-253. https://doi.org/https://doi.org/10.1006/jcis.1993.1182

Tanudjaja, H. J., Hejase, C. A., Tarabara, V. V., Fane, A. G., & Chew, J. W. (2019). Membrane-based separation for oily wastewater: A practical perspective. *Water Research*, *156*, 347-365. https://doi.org/https://doi.org/10.1016/j.watres.2019.03.021

Tanudjaja, H. J., Tarabara, V. V., Fane, A. G., & Chew, J. W. (2017). Effect of cross-flow velocity, oil concentration and salinity on the critical flux of an oil-in-water emulsion in microfiltration. *Journal of Membrane Science*, *530*, 11-19. https://doi.org/https://doi.org/10.1016/j.memsci.2017.02.011

Trinh, T. A., Han, Q., Ma, Y., & Chew, J. W. (2019). Microfiltration of oil emulsions stabilized by different surfactants. *Journal of Membrane Science*, *579*, 199-209. https://doi.org/https://doi.org/10.1016/j.memsci.2019.02.068

Tummons, E., Han, Q., Tanudjaja, H. J., Hejase, C. A., Chew, J. W., & Tarabara, V. V. (2020). Membrane fouling by emulsified oil: A review. *Separation and Purification Technology*, *248*, 116919. https://doi.org/https://doi.org/10.1016/j.seppur.2020.116919

Tummons, E. N., Chew, J. W., Fane, A. G., & Tarabara, V. V. (2017). Ultrafiltration of saline oil-in-water emulsions stabilized by an anionic surfactant: Effect of surfactant concentration and divalent counterions. *Journal of Membrane Science*, *537*, 384-395. https://doi.org/https://doi.org/10.1016/j.memsci.2017.05.012

Ullah, A., Tanudjaja, H. J., Ouda, M., Hasan, S. W., & Chew, J. W. (2021). Membrane fouling mitigation techniques for oily wastewater: A short review. *Journal of Water Process Engineering*, *43*, 102293. https://doi.org/https://doi.org/10.1016/j.jwpe.2021.102293

Virga, E., Bos, B., Biesheuvel, P. M., Nijmeijer, A., & de Vos, W. M. (2020). Surfactant-dependent critical interfacial tension in silicon carbide membranes for produced water treatment. *Journal of Colloid and Interface Science*, *571*, 222-231. https://doi.org/https://doi.org/10.1016/j.jcis.2020.03.032

Wang, X., Sun, K., Zhang, G., Yang, F., Lin, S., & Dong, Y. (2022). Robust zirconia ceramic membrane with exceptional performance for purifying nano-emulsion oily wastewater. *Water Research*, *208*, 117859. https://doi.org/https://doi.org/10.1016/j.watres.2021.117859

Wenzlick, M., & Siefert, N. (2020). Techno-economic analysis of converting oil & gas produced water into valuable resources. *Desalination*, *481*, 114381. https://doi.org/https://doi.org/10.1016/j.desal.2020.114381

Xu, M., Xu, C., Rakesh, K. P., Cui, Y., Yin, J., Chen, C., Wang, S., Chen, B., & Zhu, L. (2020). Hydrophilic SiC hollow fiber membranes for low fouling separation of oil-in-water emulsions with high flux [10.1039/C9RA06695K]. *RSC Advances*, *10*(8), 4832-4839. https://doi.org/10.1039/C9RA06695K

Yan, L., Li, P., Zhou, W., Wang, Z., Fan, X., Chen, M., Fang, Y., & Liu, H. (2019). Shrimp Shell-Inspired Antifouling Chitin Nanofibrous Membrane for Efficient Oil/Water Emulsion Separation with In Situ Removal of Heavy Metal Ions. *ACS Sustainable Chemistry & Engineering*, *7*(2), 2064-2072. https://doi.org/10.1021/acssuschemeng.8b04511

Yu, W., Liu, M., & Graham, N. J. D. (2019). Combining Magnetic Ion Exchange Media and Microsand before Coagulation as Pretreatment for Submerged Ultrafiltration: Biopolymers and Small Molecular Weight Organic Matter. *ACS Sustainable Chemistry & Engineering*, *7*(22), 18566-18573. https://doi.org/10.1021/acssuschemeng.9b04678

Zhang, Q., Fan, Y., & Xu, N. (2009). Effect of the surface properties on filtration performance of Al2O3–TiO2 composite membrane. *Separation and Purification Technology*, *66*(2), 306-312. https://doi.org/https://doi.org/10.1016/j.seppur.2008.12.010

Zhou, J.-e., Chang, Q., Wang, Y., Wang, J., & Meng, G. (2010). Separation of stable oil–water emulsion by the hydrophilic nano-sized ZrO2 modified Al2O3 microfiltration membrane. *Separation and Purification Technology*, *75*(3), 243-248. https://doi.org/https://doi.org/10.1016/j.seppur.2010.08.008

Appendix

	Al_2O_3 ceramic membrane					SiC-deposited membrane				
pH 4	absorbance(A)	Rejection(%)	COD(mg/L)		Rejection(100%)	absorbance(A)	Rejection(%)	COD(mg/L)		Rejection(%)
feed	1.759		1973	1994		1.778		1787	1825	
1	0.056	96.81637294	39.2	34.4	98.14469372	0.016	99.10011249	52.3	49.7	97.17607973
2	0.023	98.69243889	33.7	32.8	98.32367028	0.003	99.83127109	41.9	39.8	97.73809524
3	0.018	98.9766913	40.6	41.7	97.92538442	0.008	99.55005624	31.3	34.6	98.17552602
4	0.01	99.43149517	48.2	44.4	97.66574237	0.018	98.98762655	36.7	37.4	97.94850498
5	0.009	99.48834565	54.8	52	97.30778926	0.012	99.32508436	38.5	40.1	97.82392027
6	0.005	99.71574758	53.4	50.6	97.37837157	0.008	99.55005624	41.3	42.9	97.66888151
pH 6	absorbance(A)	Rejection(%)	COD(mg/L)		Rejection(100%)	absorbance(A)	Rejection(%)	COD(mg/L)		Rejection(%)
feed	1.717		1818	1763		1.747		1997	2070	
1	0.017	99.00990099	75.6	74.3	95.81401843	0.029	98.34001145	50.3	50.3	97.52643226
2	0.021	98.77693652	73.7	77	95.7916783	0.036	97.93932456	43.9	48.9	97.71821982
3	0.014	99.18462434	77.5	76.4	95.70231779	0.011	99.37034917	45.6	49.6	97.65920826
4	0.014	99.18462434	80	77.6	95.59899469	0.011	99.37034917	49.1	44.8	97.69117285
5	0.011	99.3593477	79.5	75	95.68556269	0.01	99.42759015	51.5	46.6	97.58790263
6	0.012	99.30110658	77.4	76.5	95.70231779	0.018	98.96966228	46.7	47.5	97.68379641
pH 8	absorbance(A)	Rejection(%)	COD(mg/L)		Rejection(100%)	absorbance(A)	Rejection(%)	COD(mg/L)		Rejection(%)
feed	1.984		1749	1852		1.981		1708	1697	
1	0.011	99.44556452	74.7	78.6	95.74284921	0.023	98.83897022	50.7	50.9	97.01615272
2	0.012	99.39516129	75	79.2	95.71785615	0.025	98.73801111	51.5	49	97.04845815
3	0.001	99.94959677	72.6	71	96.01221883	0.007	99.64664311	52.3	53.3	96.89867841
4	0.007	99.64717742	68.2	72.2	96.10108303	0.019	99.04088844	43.3	46	97.3773862
5	0.008	99.59677419	77.6	70.6	95.88447653	0.019	99.04088844	47.3	44.7	97.29809104
6	0.01	99.49596774	68.8	75.7	95.98722577	0.021	98.93992933	54.5	60.4	96.62555066
Span 80 + Tween 80	absorbance(A)	Rejection(%)	COD(mg/L)		Rejection(100%)	absorbance(A)	Rejection(%)	COD(mg/L)		Rejection(%)
feed	1.559		1772	1709		1.522		1479	1440	
1	0.006	99.61513791	39	42.8	97.65010055	0.002	99.86859396	21.4	22.7	98.48920863
2	0.003	99.80756895	27.1	29.7	98.36828498	0.004	99.73718791	26.2	28.2	98.13634806
3	0.001	99.93585632	24.4	22.7	98.64694053	0.003	99.80289093	22.5	25.7	98.34874957
4	0.013	99.16613214	22.3	21.9	98.73024993	0.005	99.67148489	20.3	21.5	98.56800274
5	0.007	99.55099423	27.4	27.9	98.41137604	0.013	99.14586071	16.5	24.6	98.59198356
6	0.005	99.67928159	23.4	24.6	98.62108589	0.011	99.27726675	22.3	19.2	98.57828023
Span 80 + CTAB	absorbance(A)	Rejection(%)	COD(mg/L)		Rejection(100%)	absorbance(A)	Rejection(%)	COD(mg/L)		Rejection(%)
feed	1.749		1923	1889		1.744		1819	1797	
1	0.024	98.62778731	37.8	36.9	98.04039874	0.021	98.79587156	35	33.5	98.10564159
2	0.015	99.14236707	39	37.5	97.99317943	0.023	98.68119266	39.5	42.3	97.73783186
3	0.007	99.5997713	40.6	38.8	97.91710388	0.015	99.13990826	39	38.4	97.85951327
4	0.006	99.65694683	44.4	41.6	97.74396642	0.011	99.36926606	39	37.8	97.87610619
5	0.006	99.65694683	39.7	38.4	97.95120672	0.01	99.4266055	38.3	38	97.88993363
6	0.001	99.94282447	42.1	42	97.79380902	0.022	98.73853211	39.9	37.5	97.85951327
Span80 + SDS	absorbance(A)	Rejection(%)	COD(mg/L)		Rejection(100%)	absorbance(A)	Rejection(%)	COD(mg/L)		Rejection(%)
feed	1.717		1818	1763		1.747		1997	2070	
1	0.017	99.00990099	75.6	74.3	95.81401843	0.029	98.34001145	50.3	50.3	97.52643226
2	0.021	98.77693652	73.7	77	95.7916783	0.036	97.93932456	43.9	48.9	97.71821982
3	0.014	99.18462434	77.5	76.4	95.70231779	0.011	99.37034917	45.6	49.6	97.65920826
4	0.014	99.18462434	80	77.6	95.59899469	0.011	99.37034917	49.1	44.8	97.69117285
5	0.011	99.3593477	79.5	75	95.68556269	0.01	99.42759015	51.5	46.6	97.58790263
6	0.012	99.30110658	77.4	76.5	95.70231779	0.018	98.96966228	46.7	47.5	97.68379641
1mM NaCl	absorbance(A)	Rejection(%)	COD(mg/L)		Rejection(100%)	absorbance(A)	Rejection(%)	COD(mg/L)		Rejection(%)
feed	1.787		1889	1917		1.839		1977	1947	
1	0.011	99.3844432	67.7	64.2	96.53441934	0.016	99.12996194	54.8	53.9	97.22986748
2	0.002	99.88808058	73.7	72.9	96.14818707	0.016	99.12996194	54.4	55.6	97.19673802
3	0.01	99.44040291	66.3	67.2	96.49238045	0.018	99.02120718	53.3	54.1	97.26299694
4	0.01	99.44040291	71.3	72.3	96.22700998	0.011	99.40184883	51.3	51.9	97.37003058
5	0.008	99.55232233	67.2	66.9	96.47661587	0.012	99.34747145	55.2	57.1	97.13812436
6	0.009	99.49636262	70.2	70.9	96.29269574	0.012	99.34747145	53.7	54.1	97.25280326
10mM NaCl	absorbance(A)	Rejection(%)	COD(mg/L)		Rejection(100%)	absorbance(A)	Rejection(%)	COD(mg/L)		Rejection(%)
feed	1.749		1876	1843		1.744		1799	1822	
1	0.024	98.62778731	36.8	37.4	98.00484001	0.021	98.79587156	37.1	36.7	97.96188898
2	0.015	99.14236707	37.9	37.5	97.97257327	0.023	98.68119266	37.6	37.9	97.91494062
3	0.007	99.5997713	39.4	40.2	97.85963969	0.015	99.13990826	36.7	36.2	97.98674399
4	0.006	99.65694683	41.2	41.6	97.77359505	0.011	99.36926606	36.8	37.2	97.95636564
5	0.006	99.65694683	39.6	40.2	97.8542619	0.01	99.4266055	37.9	38.1	97.90113228
6	0.001	99.94282447	37.5	38.2	97.96450659	0.022	98.73853211	39.4	39.1	97.83209058
1mM NaCl + 1mM $CaCl_2$	absorbance(A)	Rejection(%)	COD(mg/L)		Rejection(100%)	absorbance(A)	Rejection(%)	COD(mg/L)		Rejection(%)
feed	1.717		1942	1937		1.747		1947	1939	
1	0.017	99.00990099	40.9	41.2	97.88347512	0.029	98.34001145	49.1	49.7	97.45753989
2	0.021	98.77693652	38.7	39.1	97.99432844	0.036	97.93932456	48.1	47.2	97.54760679
3	0.014	99.18462434	41.2	40.7	97.88863109	0.011	99.37034917	51.7	51.2	97.35203294
4	0.014	99.18462434	37.9	38.2	98.03815416	0.011	99.37034917	48.9	49.4	97.47040659
5	0.011	99.3593477	41.2	41.9	97.85769528	0.01	99.42759015	49.8	50.9	97.40864642
6	0.012	99.30110658	38.9	39.2	97.98659448	0.018	98.96966228	46.9	46.8	97.58878024

Fig. S 1. Oil rejection calculation based on UV/Vis and COD data for all the nano-sized O/W emulsion separation experiments.

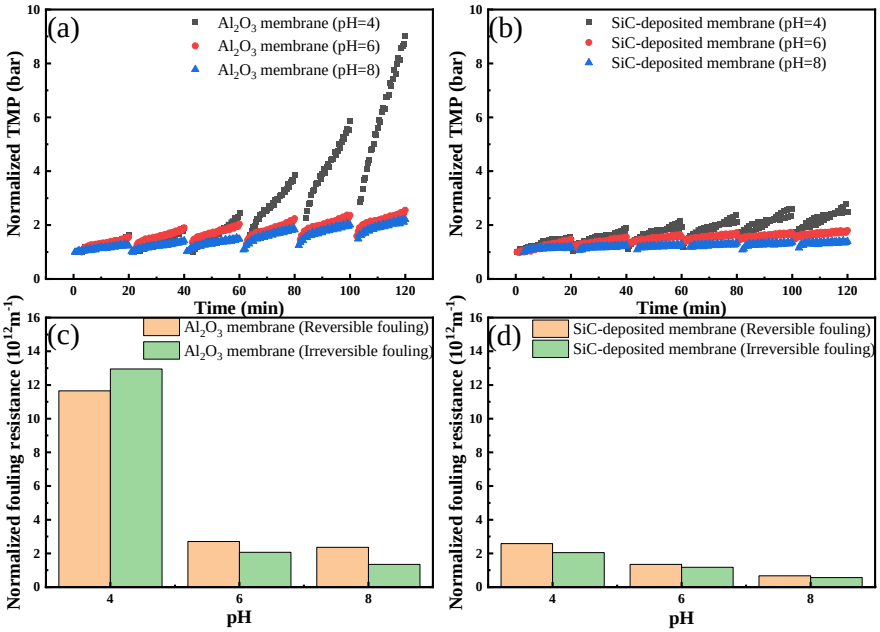

Fig. S 2. The normalized TMP curve and the normalized fouling resistance curve for the SiC-deposited membrane and the Al_2O_3 membrane in different pH conditions: (a) The normalized TMP of the Al_2O_3 membrane dealing with Span 80/SDS-stabilized nanoemulsions under different pH conditions, (b) The normalized TMP of the SiC-deposited membrane dealing with Span 80/SDS-stabilized nanoemulsions under different pH conditions, (c) The normalized fouling resistance of the Al_2O_3 membrane dealing with Span 80/SDS-stabilized nanoemulsions under different pH conditions, and (d) The normalized fouling resistance of the SiC-deposited membrane dealing with Span 80/SDS-stabilized nanoemulsions under different pH conditions.

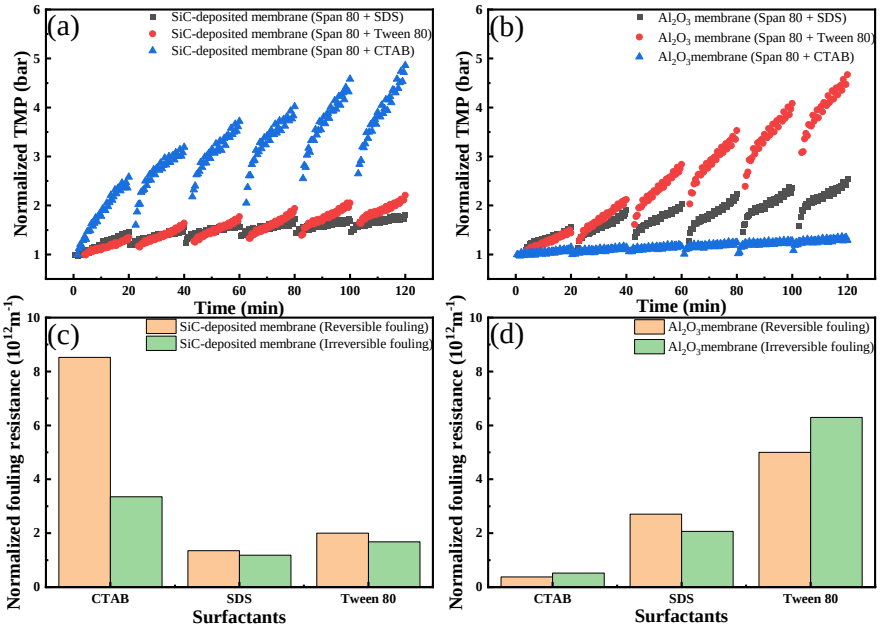

Fig. S 3. The normalized TMP curve and the normalized fouling resistance curve for the SiC-deposited membrane and the Al_2O_3 membrane dealing with 500 mg/L nano-sized O/W emulsions stabilized with different surfactants: (a) The normalized TMP of the Al_2O_3 membrane dealing with Span 80/SDS-stabilized nanoemulsions under different surfactant conditions, (b) The normalized TMP of the SiC-deposited membrane dealing with Span 80/SDS-stabilized nanoemulsions under different surfactant conditions, (c) The normalized fouling resistance of the Al_2O_3 membrane dealing with Span 80/SDS-stabilized nanoemulsions under different surfactant conditions, and (d) The normalized fouling resistance of the SiC-deposited membrane dealing with Span 80/SDS-stabilized nanoemulsions under different surfactant conditions..

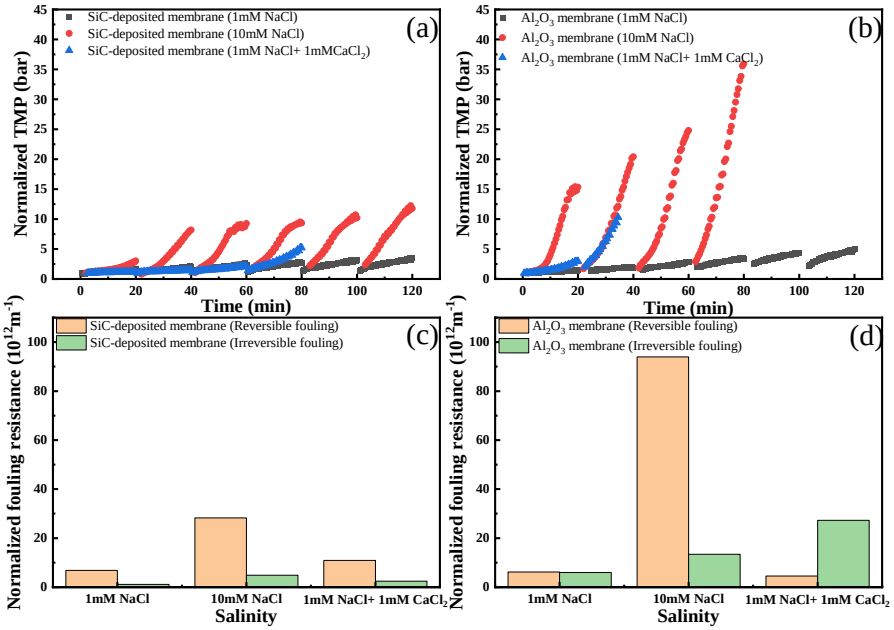

Fig. S 4. The normalized TMP curve and the normalized fouling resistance curve for the SiC-deposited membrane and the Al_2O_3 membrane in different salinity conditions: (a) The normalized TMP of the Al_2O_3 membrane dealing with Span 80/SDS-stabilized nanoemulsions under different salinity conditions, (b) The normalized TMP of the SiC-deposited membrane dealing with Span 80/SDS-stabilized nanoemulsions under different salinity conditions, (c) The normalized fouling resistance of the Al_2O_3 membrane dealing with Span 80/SDS-stabilized nanoemulsions under different salinity conditions, and (d) The normalized fouling resistance of the SiC-deposited membrane dealing with Span 80/SDS-stabilized nanoemulsions under different salinity conditions.

Name	Mean (mV)	Satndard deviation (mV)
Tween 80/Span 80-stablized nanoemulsion	-21.3	0.73
CTAB/Span 80-stablized nanoemulsion	62.67	0.76
SDS/Span 80-stablized nanoemulsion (pH = 6)	-58.3	0.82
SDS/Span 80-stablized nanoemulsion with 1 mM NaCl	-50.1	0.41
SDS/Span 80-stablized nanoemulsion with 10 mM NaCl	-42.8	0.86
SDS/Span 80-stablized nanoemulsion with 1 mM NaCl and 1mM $CaCl_2$	-38.2	0.65
SDS/Span 80-stablized nanoemulsion (pH = 4)	-55.6	0.86
SDS/Span 80-stablized nanoemulsion (pH = 8)	-60.3	1.64

Table. S 1. The zeta potential of O/W nanoemulsions with various pH, salinity and surfactant.

Name	MV(μm)	MN(μm)	MA(μm)
Span 80/SDS-stablized nanoemulsion	147	69	108
Span 80/Tween 80-stablized nanoemulsion	143	61	104
Span 80/CTAB-stablized nanoemulsion	142	81	113

Table. S 2. The average size of the nanoemulsion stabilized with Span 80/SDS, Span 80/Tween 80 and Span 80/CTAB.